ORIGINAL PAPER

Electrochemical behavior of Ti-20Cr-X alloys in artificial saliva containing fluoride

Wen-Fu Ho · Shih-Ching Wu · Cheng-Wei Lin ·
Shih-Kuang Hsu · Hsueh-Chuan Hsu

Abstract In this study, electrochemical investigation was carried out on commercially pure titanium (c.p. Ti) and as-cast Ti-20Cr-X (X = Nb, Mo, Fe, and Cr) in fluoride solutions containing artificial saliva. Open-circuit potential (OCP) and potentiodynamic polarization measurement were used to characterize the electrochemical behavior, and X-ray photoelectron spectroscopy (XPS) was used to characterize the composition of the passive films on the samples. The OCP results indicated that all specimens presented spontaneous passivation. XPS results showed that pre-test, a passive film consisting of TiO_2 and Cr_2O_3 formed on the surface of the Ti-20Cr-X alloys, and Na_2TiF_6 formed on the surface of all specimens after the polarization test in artificial saliva with 0.5 wt% NaF. Although the Ti-20Cr-X alloys exhibited a Na_2TiF_6 film on their surface, their corrosion rate was still lower than that of c.p. Ti. In particular, Ti-20Cr-Mo alloy exhibited the lowest steady state current density compared to c.p. Ti and the other Ti-20Cr-X alloys. All these results suggest that the Ti-20Cr-X alloys hold promise for application as dental materials in a natural oral environment where NaF may be present.

W.-F. Ho
Department of Materials Science and Engineering,
Dayeh University, Changhua, Taiwan, ROC

S.-C. Wu · S.-K. Hsu · H.-C. Hsu (✉)
Department of Dental Technology and Material Science, Central Taiwan University of Science and Technology, No. 666, Buzih Road, Beitun District, Taichung 40601, Taiwan, ROC
e-mail: hchsu@ctust.edu.tw

S.-C. Wu · C.-W. Lin · S.-K. Hsu · H.-C. Hsu
Institute of Biomedical Engineering and Material Science,
Central Taiwan University of Science and Technology,
Taichung, Taiwan, ROC

1 Introduction

Many titanium alloys have been developed for dental crowns and bridges, dental implants, and orthopedic applications [1–3], and their properties have been extensively studied, mainly to improve the strength and castability of titanium [1, 4–7]. To improve the mechanical properties or corrosion resistance of pure metals or known alloys, new alloys are constantly being developed through the addition of different elements to a given metal. Ti–Cr alloys in particular have previously been developed for dental applications [8, 9], with the β-isomorphous elements (Nb, Zr, and Mo) and β-eutectoid elements (Cr and Fe) all being used [10]. Among these, β-titanium alloys are shown to be the most versatile, and a number of studies have been performed on them [11]. Previous work by the authors [12] showed that Ti-20Cr was comprised entirely of a bcc β phase, and when 1 wt% Nb, Mo, Zr or Fe was added, the microstructure was similar to that of the Ti-20Cr alloy with equi-axed grain structures. Under optical microscopy, Ti-20Cr and the Ti-20Cr-X alloys displayed typical etched microstructures. However, while these Ti-20Cr-X alloys have been shown to have better mechanical properties than c.p. Ti [12], their corrosion resistance behavior requires further investigation. Recently, several authors have found that an experimental Ti alloy containing 20 mass% chromium showed superior corrosion resistance in a saline solution containing fluoride [16–18]. Thus, the purpose of this study was to evaluate the corrosion behavior of four kinds of ternary cast Ti alloys, including Ti-20Cr-1Nb, Ti-20Cr-1Mo, Ti-20Cr-1Zr, and Ti-20Cr-1Fe in simulated

oral environments with and without fluoride. For this purpose, c.p. Ti was used as the control.

A number of researchers have reported the negative influence of fluoride on the corrosion resistance of Ti [13–18]. Ti and its alloys are widely used in the dental field, and since the oral environment is exposed to fluoride, the degree of corrosion resistance offered by these metals in a fluoride-containing medium has become an important property for their use in dentistry. It has been reported that the fluoride concentration (in terms of NaF) in some commercial toothpastes or prophylactic gels vary from 0.1 to 2 wt% [13], and for this reason, different concentrations of NaF were chosen to assess the influence of fluoride on the corrosion of Ti alloys in the present study.

2 Experimental procedure

2.1 Specimen preparation

The Ti-20Cr alloy and a series of Ti alloys, including Ti-20Cr-1Nb, Ti-20Cr-1Mo, Ti-20Cr-1Zr, and Ti-20Cr-1Fe, were prepared from 99.8% pure titanium, using a commercial arc-melting vacuum-pressure-type casting system (Castmatic, Iwatani Corp., Japan). Alloying elements selected for the study include Cr, Nb, Mo, Zr, and Fe, which were all 99.9% pure. For the electrochemical measurement, specimens were cut to a thickness of 1.0 mm from a rod. The specimens were ground with silicon carbide paper until #1500 and then polished with 0.3 μm Al_2O_3 suspension. After polishing, the samples were ultrasonically cleaned in ethanol.

2.2 Electrochemical tests

In this study, the corrosion behavior of Ti-20Cr-X alloys was evaluated using artificial saliva as the base electrolyte to which varying concentrations of NaF (0.1 and 0.5 wt%) were added to study the influence of fluoride. The choice of this base electrolyte was based on a previous report by Hsu et al. [19], and the composition of the artificial saliva was (NaCl 400 mg L^{-1}, KCl 400 mg L^{-1}, $CaCl_2 \cdot 2H_2O$ 795 mg L^{-1}, $NaH_2PO_4 \cdot H_2O$ 690 mg L^{-1}, KSCN 300 mg L^{-1}, $Na_2S \cdot 9H_2O$ 5 mg L^{-1}, and urea 1000 mg L^{-1}). The pH level of the test solution was adjusted to 4.0 by adding lactic acid in a simulated oral environment. A three-electrode system was used for all the electrochemical measurements. The apparatus for electrochemical measurement consisted of a potentiostat (Versa Stat TM [II] Potentiostat/Golvanostat Model 263A; Princeton Applied Research, NJ, USA), controlled by a personal computer with dedicated software (PowerSuit-2.56, Princeton Applied Research), a saturated calomel electrode (SCE) as reference electrode, a platinum plate as counter electrode, and the specimen as working electrode. For each test, the open-circuit potential (OCP) was measured for 2 h. The potentiodynamic polarization of the specimens was recorded in a scanning range from −1.2 to +2.5 V (vs. SCE) at a scanning rate of 0.1 mV s^{-1}. In every test, the medium was maintained at 37 °C. Five specimens were tested for each condition.

2.3 Surface characterization

Surface morphology of specimens was examined using a scanning electron microscope (S-3000 N, HITACHI, Japan), and the passive films were examined with XPS (Shimadzu, Japan). The specimens were prepared for SEM and XPS by applying the potential of 0.5 V versus SCE for 2 h.

3 Results and discussion

3.1 OCP analyses

Figures 1, 2, 3 show the changes in OCP of c.p. Ti and Ti-20Cr-X alloys over a period of 2 h in standard saliva solution with different NaF concentrations (0, 0.1, and 0.5 wt%). The results obtained from the OCP measurements in standard artificial saliva without NaF are presented in Fig. 1. These indicate that the potential gradually shifts toward the negative, until it reaches a steady-state. Although the time profiles of the OCP obtained for all samples in this solution were similar, the Ti-20Cr-X alloys, particularly Ti-20Cr-Mo (−473 mV) showed more positive OCP values than c.p Ti (−624 mV). This change of potential profile indicates that all the alloys as well as c.p. Ti undergo spontaneous passivation in the electrolyte
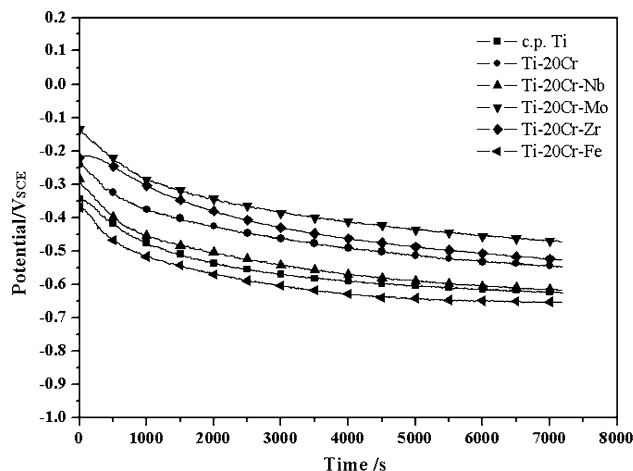

Fig. 1 OCP of c.p. Ti and Ti-20Cr-X alloys in standard artificial saliva

solution. On the whole, these results indicate that the spontaneous oxide film formed on the Ti-20Cr-Mo alloy displays better corrosion protection characteristics than those found on c.p. Ti and the other Ti-20Cr-X alloys.

In contrast with the alloys, the OCP of c.p., Ti dropped rapidly to −1065 mV at 5000 s in 0.1 wt% NaF artificial saliva (Fig. 2). A similar result was found in 0.5 wt% NaF artificial saliva, although the OCP of c.p. Ti decreased to −1195 mV at 3000 s (Fig. 3). As shown in Figs. 2 and 3, there is a marked difference between the OCP of c.p. Ti in saliva solutions of 0.1 and 0.5 wt% NaF, with the OCP of c.p. Ti in 0.5 wt% NaF dropping more rapidly. Thus, as the NaF concentration is increased, the OCP curve drops sooner and more sharply and it seems clear that the corrosion behavior of c.p. Ti is directly affected by fluoride concentration. In fact, Nakagawa et al. and Robin et al.

[14, 20] found similar results for c.p. Ti and the Ti-6Al-4 V alloy.

The OCP curves for Ti-20Cr-X in artificial saliva with 0.1 and 0.5 wt% NaF are shown Figs. 2 and 3. In the 0.1 wt% NaF solution, these decreased gradually before finally stabilizing. In this solution, Ti-20Cr-X alloys, particularly Ti-20Cr-Mo (−677 mV) showed higher stable potentials (−677 to −814 mV) than that of c.p. Ti (−1087 mV). Comparing the results obtained in 0.1 and 0.5 wt% NaF solutions (Figs. 2, 3), though the time profiles were similar for the Ti-20Cr-X alloys, the final potential had decreased, and ranged from −767 to −838 mV in the saliva solution with 0.5 wt% NaF compared for 0.1 wt% NaF. Despite the fact that the Ti-20Cr and Ti-20Cr-X alloys showed more tendency to spontaneously form surface oxides than c.p. Ti, they were still affected by fluoride concentration.

3.2 Potentiodynamic polarization studies of the Ti alloys

The potentiodynamic polarization curves of c.p. Ti and Ti-20Cr-X alloys in artificial saliva without NaF, and with 0.1 and 0.5 wt% NaF are shown in Fig. 4, 5, 6. All the specimens had distinct and long passive regions in standard artificial saliva, as shown in Fig. 4. Significantly, the average corrosion potentials estimated from the linear polarization curves (−912 to −1073 mV) were significantly lower than those obtained from the OCP measurements (−473 to −654 mV). This is because the polarization tests were started at a cathodic potential close to the corrosion potential, and the passive film on the surface was subtracted [19]. Furthermore, this study has shown that alloying elements (Nb, Mo, Zr, and Fe) can shift an alloy's corrosion potential to more noble values, especially in the case of Ti-20Cr-Mo,
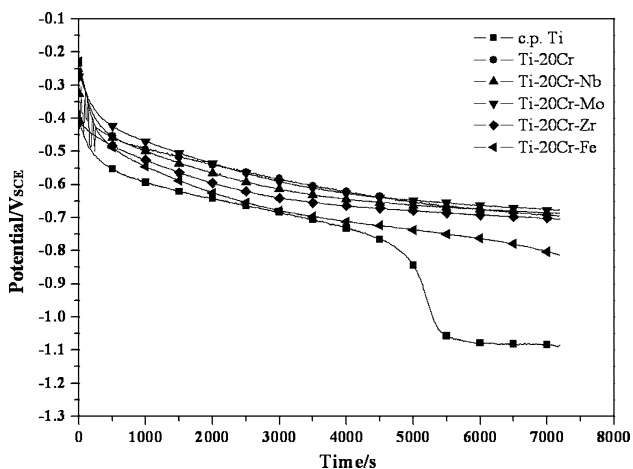

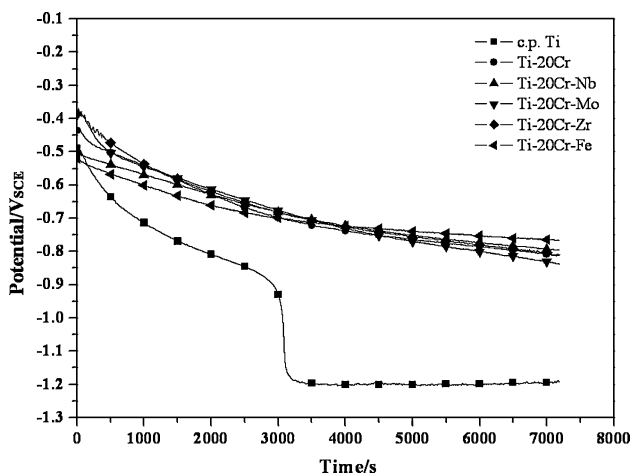**Fig. 2** OCP of c.p. Ti and Ti-20Cr-X alloys in saliva solution with 0.1 wt% NaF

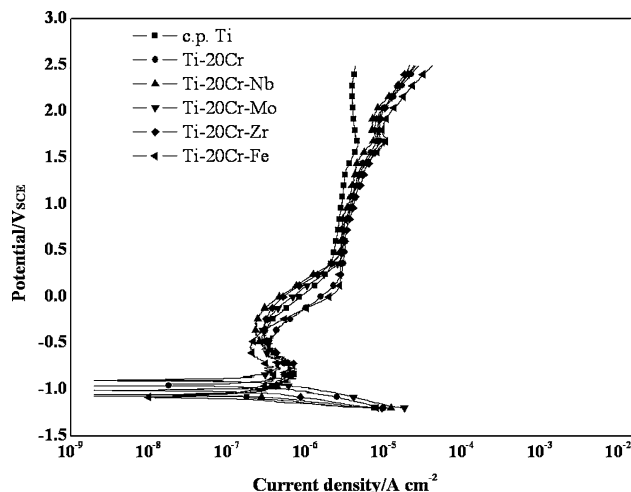**Fig. 3** OCP of c.p. Ti and Ti-20Cr-X alloys in saliva solution with 0.5 wt% NaF

Fig. 4 Dynamic polarization diagrams of c.p. Ti and Ti-20Cr-X alloys in the standard artificial saliva
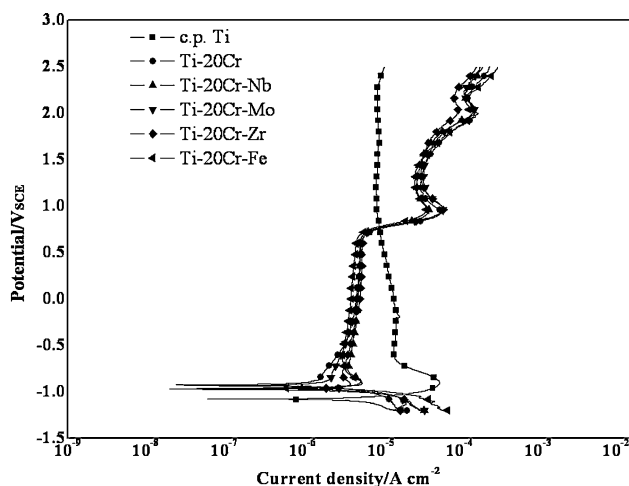
Fig. 5 Dynamic polarization diagrams of c.p. Ti and Ti-20Cr-X alloys in the standard artificial saliva with 0.1 wt% NaF
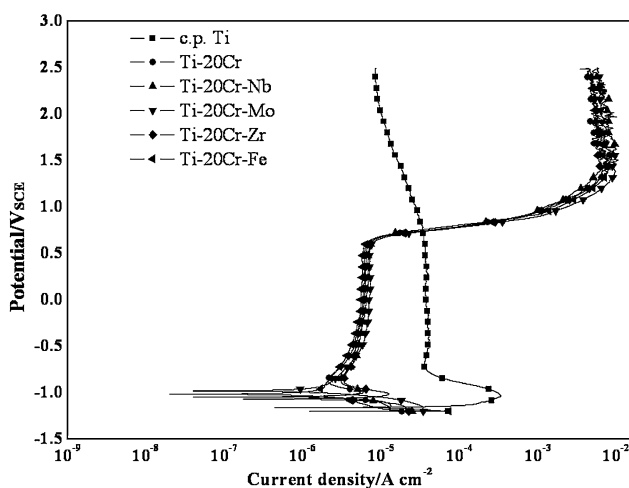

Fig. 6 Dynamic polarization diagrams of c.p. Ti and Ti-20Cr-X alloys in the standard artificial saliva with 0.5 wt% NaF

where the strong shift in the positive direction indicates that the corrosion resistance of Ti-20Cr-Mo is superior to those of other Ti-20Cr-X alloys.

The polarization curves in the 0.1 wt% NaF solution are shown in Fig. 5, and there is a clear difference in the corrosion potentials between Ti-20Cr, Ti-20Cr-X alloys and c.p. Ti. For Ti-20Cr and Ti-20Cr-X alloys ($I_{0.5V} = 4.6$–5.8 μA cm^{-2}), lower passive current densities were observed as compared to c.p. Ti ($I_{0.5V} = 10.6$ μA cm^{-2}). There was also a difference between Ti-20Cr-X alloys and c.p. Ti in 0.5 wt% NaF artificial saliva (Fig. 6). Again, lower passive current densities were observed for Ti-20Cr and all Ti-20Cr-X alloys ($I_{0.5V} = 6.3$–6.9 μA cm^{-2}) as compared to c.p. Ti ($I_{0.5V} = 39.9$ μA cm^{-2}). Although the presence of NaF in the artificial saliva did not hinder the formation of

passive oxide film on the surface of any of the Ti alloys, the active region of the polarization curves of all the Ti alloys was extended in the presence of NaF. This apparent negative influence of fluoride on the corrosion resistance of these Ti alloys is also confirmed by other research [21–23]. For all the specimens analyzed in this study, in the given potential regions where the current remains constant, the passive currents are relatively low, indicating that the oxide films formed under these conditions confer good protection to the metal substrate.

In contrast with c.p. Ti, the polarisation curves of Ti-20Cr and Ti-20Cr-X alloys broke down after reaching a passive region, resulting in a distinctly shorter passive region, as shown in Figs. 5 and 6. Given that the potential in a natural oral environment is generally between −0.3 and +0.3 V [24], the Ti-20Cr-X alloys, and similarly, the Ti-20Cr alloy would most likely not dissolve in such an environment.

For all the Ti alloys studied, the average passive current density is lower than that of c.p. Ti, and there is little variation in the average passive current density of Ti-20Cr-X alloys in artificial saliva containing either 0.1 or 0.5 wt% NaF. However, in artificial saliva containing 0.5 wt% NaF in particular, the average passive current density of the Ti-20Cr-X alloys is significantly lower than that of c.p. Ti. This can be attributed to the precipitation of chromium oxide, along with the oxides of Ti on the surface of the Ti-20Cr-X alloys. Therefore, to get more insight into the corrosion behavior of these Ti alloys, XPS studies were also performed.

3.3 Surface characterization

Figure 7 shows Cr 2p, Ti 2p, O 1 s and F 1 s XPS spectra of all Ti specimens after electrochemical measurement in artificial saliva containing 0.5 wt% NaF. The XPS spectrum of Ti 2p showed two peaks, at 458.8 and 464.2 eV (Fig. 7a). For the most part, all specimens showed a Ti^{4+} state. The XPS spectrum of Cr 2p showed two peaks (at 573.8 and 576.7 eV) (Fig. 7b). All Ti-20Cr and Ti-20Cr-X alloys showed Cr^{3+} peaks in the Cr 2p region. The XPS spectrum of O 1 s showed a single peak at 530.5 eV (Fig. 7c). All the specimens predominantly showed an O^{2-} state, and it is evident that the surface of the samples consisted of TiO_2 for c.p. Ti, and both TiO_2 and Cr_2O_3 for Ti-20Cr and Ti-20Cr-X alloys. In addition, the F 1 s peak at 685.3 eV demonstrates the presence of Na_2TiF_6, as shown in Fig. 7d. These results are consistent with Ti dissolving to form Na_2TiF_6, because F^- shifts the anodic dissolution curve to higher currents and promotes active dissolution by forming TiF_6^{2-}, which is more stable than TiO_2 [22]. Furthermore, since Na_2TiF_6 is not
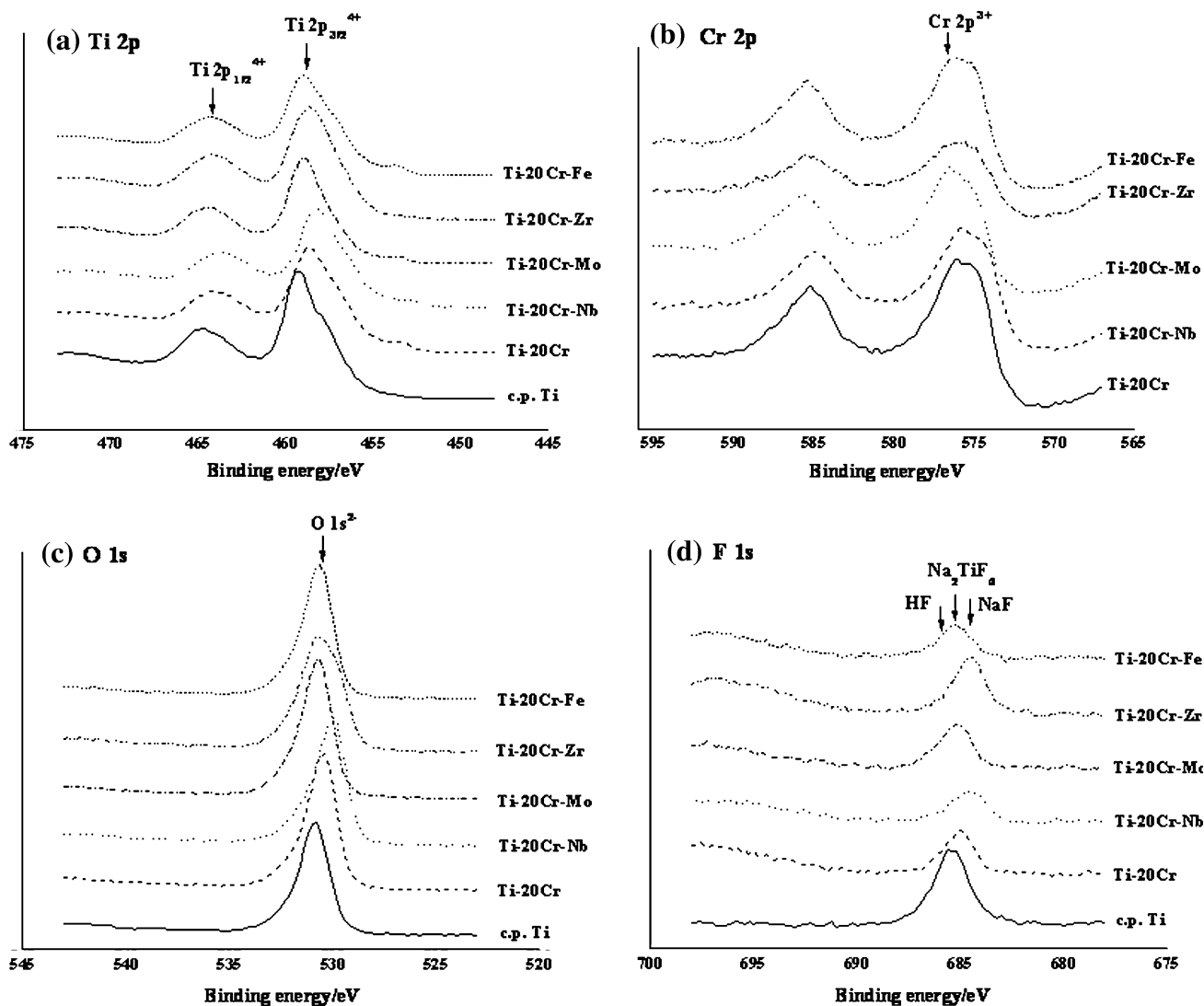
Fig. 7 XPS spectra of all titanium specimens after applying the potential of 0.5 V versus SCE in artificial saliva containing 0.5 wt% NaF. **a** Ti 2p; **b** Cr 2p; **c** O 1 s; **d** F 1 s

protective, the corrosion resistance of Ti alloys is adversely affected. Significantly, Fig. 7d shows that the intensity of F 1 s peak (Na_2TiF_6) for c.p. Ti was higher than that of the Ti-20Cr and Ti-20Cr-X alloys, which means that a lower amount of Na_2TiF_6 was formed on the surface of the Ti-20Cr-X alloys than on the c.p. Ti.

Figure 8a–e are the SEM images of all the samples after applying the potential of 0.5 V versus SCE for 2 h in the artificial saliva containing 0.5 wt% NaF. As shown in Fig. 8a, the surface of the c.p. Ti has become roughened and some localized corrosion has occurred. Figure 8b–f show the surfaces of the Ti-20Cr-X alloys. As seen in Fig. 8c–f, the surfaces of the samples were slightly roughened, but without any significant sign of localized damage such as that observed on the c.p. Ti. Thus, it appears that Ti-20Cr-X alloys showed a better corrosion resistance to fluoride due to the formation of chromium oxide. In this case, the existence of Cr near the surface seems to play an important role for the improvement of corrosion resistance. Similarly, Takemoto et al. [16, 17] reported that the Ti–Cr alloy improved corrosion resistance to fluoride due to the formation of a chromium-rich oxide film and the concentration of chromic species. This is also in agreement with previous findings in which Ti-20Cr-X alloys showed better corrosion resistance than that of c.p. Ti in artificial saliva containing NaF, and was especially true for the Ti-20Cr-Mo alloy [19]. These results confirm the findings presented above that the addition of Mo to pure Ti increases its corrosion resistance due to a lower current density [25].
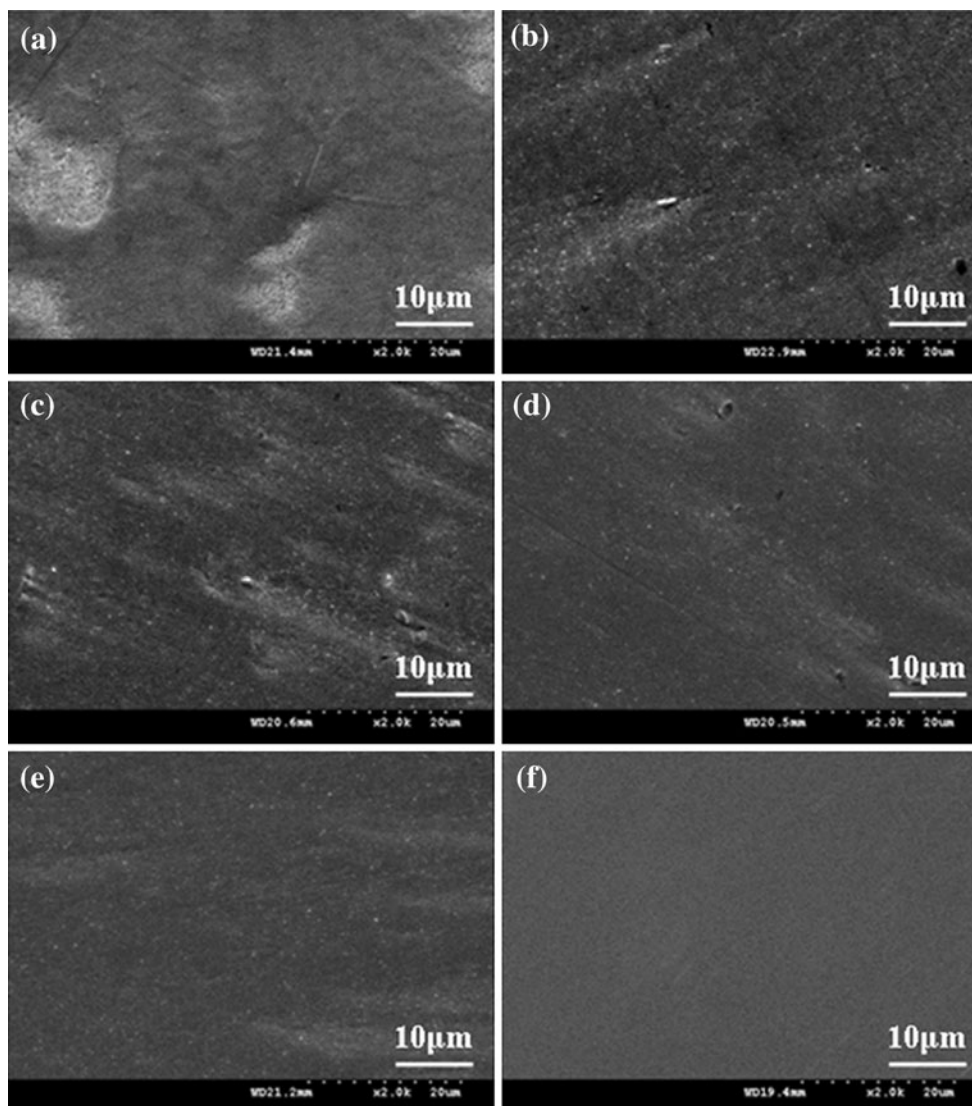
Fig. 8 SEM micrographs of all titanium specimens after applying the potential of 0.5 V versus SCE for 2 h in artificial saliva containing 0.5 wt% NaF. **a** c.p. Ti; **b** Ti-20Cr; **c** Ti-20Cr-Nb; **d** Ti-20Cr-Mo; **e** Ti-20Cr-Zr; **f** Ti-20Cr-Fe

4 Conclusions

In this study, the corrosion resistance of Ti-20Cr-X alloys and c.p. Ti were examined and compared in terms of their electrochemical corrosion behavior and surface characterization after treatment in artificial saliva solutions with and without NaF. All the Ti alloys and c.p Ti exhibit an active–passive transition in the presence of NaF, and the active region is extended to a higher current region. For all the Ti alloys, an increase in concentration of NaF increases the average passive current density. In artificial saliva with or without NaF, the Ti-20Cr-Mo alloy exhibits the lowest steady state current density compared to c.p. Ti and the other Ti-20Cr-X alloys, which is significant because it indicates a superior corrosion resistance, even in the presence of NaF, as in the natural oral environment.

References

1. Lautenschlager EP, Monaghan P (1993) Int Dent J 43:245
2. Nakajima H, Okabe T (1996) Dent Mater J 15:77
3. Wang RR, Fenton A (1996) Quintessence Int 27:401
4. Okuno O, Hamanaka H (1989) Dent Jpn 26:101
5. Hattori M, Hasegawa K, Yoshinari M, Kawada E (2001) Dent Mater J 20:16
6. Takada Y, Nakajima H, Okuno O, Okabe O (2001) Dent Mater J 20:34
7. Takahashi M, Kikuchi M, Takada Y, Okuno O (2002) Dent Mater J 21:270

8. Ho WF, Chiang TY, Wu SC, Hsu HC (2009) J Alloys Compd 474:505
9. Ho WF, Chiang TY, Wu SC, Hsu HC (2009) J Alloys Compd 468:533
10. Donachie MJ (2000) Titanium: a technical guide. ASM International, Materials Park
11. Bania PJ (1993) Beta titanium industry. In: Eylon D, Boyer RR, Koss DA (eds) Beta titanium alloys in the 1990's. TMS, Warrendale
12. Ho WF, Pan CH, Hsu HC, Wu SC (2008) J Sci Eng Tech 4:67
13. Nakagawa M, Matsuya S, Udoh K (2001) Dent Mater J 20:305
14. Nakagawa M, Matsuya S, Shiraishi T, Ohta M (1999) J Dent Res 78:1568
15. de Mele MFL, Cortizo MC (2000) J Appl Electrochem 30:95
16. Takemoto S, Hattori M, Yoshinari M, Kawada E, Asami K, Oda Y (2004) Dent Mater J 23:379
17. Takemoto S, Hattori M, Yoshinari M, Kawada E, Asami K, Oda Y (2009) Dent Mater 25:467
18. Noguchi T, Takemoto S, Hattori M, Yoshinari M, Kawada E, Oda Y (2008) Dent Mater J 27:117
19. Hsu HC, Wu SC, Wang CF, Ho WF (2009) J Alloys Compd 487:439
20. Robin A, Meirelis JP (2007) J Appl Electrochem 37:511
21. Reclaru L, Meyer JM (1998) Biomaterials 19:85
22. Schiff N, Grosgogeat B, Lissac M, Dalard F (2002) Biomaterials 23:1995
23. Takemoto S, Hattori M, Yoshinari M, Kawada E, Oda Y (2005) Biomaterials 26:829
24. Corso PP Jr, German RM, Simmons HD Jr (1985) J Dent Res 64:854
25. Oliveira NT, Guastaldi AC (2009) Acta Biomater 5:399